Chinese Chemical Letters 35 (2024) 108691

Contents lists available at ScienceDirect

Chinese Chemical Letters

journal homepage: www.elsevier.com/locate/cclet

Germylene-Fe complexes caused by heterometallic coupling and investigation into the 3d-4p bonding

Yingying Qin[a,b,1], Yongmei Kang[a,1], Lei Zhang[c], Jianping Sun[c], Zhijing Zhang[c], Jialei Xu[a,b], Fanlong Zeng[a], Anyang Li[a,*], Wenyuan Wang[a,*], Weiqun Shi[b,*]

[a] *Key Laboratory of Synthetic and Natural Functional Molecule of Ministry of Education, College of Chemistry and Materials Science, Northwest University, Xi'an 710127, China*

[b] *Laboratory of Nuclear Energy Chemistry, Institute of High Energy Physics, Chinese Academy of Sciences, Beijing 100049, China*

[c] *Shaanxi Coal and Chemical Industry, Xi'an 710054, China*

ARTICLE INFO

Article history:
Received 12 April 2023
Revised 1 June 2023
Accepted 13 June 2023
Available online 14 June 2023

Keywords:
Metallic bonding
Germylene
Iron
Crystal structure
σ bond
π backbond

ABSTRACT

The interpretation of heterometallic bonding nature is a basic work of inorganic chemistry. By means of intermetallic substitution of germylene anions with iron halide complexes CpFe(CO)$_2$I and β-diketiminato Fe^{II} chloride, the ferrogermylene complexes **3a**, **3b** and **4a** were synthesized and structurally characterized. The structural and IR characterizations show the presence of the Ge←Fe π backbonding in molecules **3a**, **3b** and **4a**. The computational works on frontier molecular orbitals and their comparison of energy states confirmed that σ donation and π backbonding are both weak in these molecules, despite three complexes have longer Ge-Fe bonds, whose strength decreases slightly with the degressive electron density around Fe environment in a sequence from **3a**, **3b** to **4a**.

The scientific study on heterometallic bonding nature between main group and transition metals is one of the core works in contemporary inorganic chemistry. The relatively earlier works in this field were the synthesis of coordination compounds of transition metals with the heavier carbene analogous R$_2$E: (E = Si, Ge, Sn; R = amido, alkyl, aryl) [1,2]. The latter possess the nonbonded electron pair with high s-character, and are able to act as donor–acceptor ligands in their transition metal complexes. Up to now, only a small number of complexes with metallic Ge-Fe bonds have been found. Among these compounds, the ferrogermylenes **A**, germylene→Fe complexes **B**, ferro-germylynes **C**, and ferrogermanes **D** have different bonding configurations (Scheme 1). In the known Ge-Fe molecules, the ferrogermylenes **A** were observed with relatively long Ge-Fe distances in the range of 2.41–2.50 Å [3–7]. In contrast, the coordinate bonding R$_2$Ge:→Fe in σ-donor/π-acceptor complexes **B** shows obviously short Ge-Fe distances in the range of 2.19–2.33 Å [2,8–12]. These species can also be regarded as Ge-Fe doubly bonded compounds because of their isoelectronic structure of "Ge=Fe" moiety, if the Ge←Fe backbond is taken into account. Pandey and co-workers presented a systematic theoretical study that π bonding contributions to the covalent bonding in the metallogermylenes **A** are much less than those in Fischer-type metal germylyne complexes [13–24]. In this work, a computational investigation on a model molecule of ferrogermylynes **C** with Ge-Fe multiple bond feature showed a really short Ge-Fe distance of 2.09 Å. Additionally, a ferrogermane molecule [Ph$_3$Ge–Fe(CO)(PPh$_3$)Cp] as shown in **D** has sp^3 hybridization around the Ge atom and a Ge–Fe distance of 2.38 Å, which is between the corresponding distances in **A** and **B**.

Now the experimental reports on ferrogermylenes involving the structural description are limited to only a few cases [4,5,25]. They were assembled by salt metathesis reactions between the corresponding β-diketiminato germylene chlorides and the Cp-Fe carbonylates M[FeCp(CO)$_2$] (M = Na, K). It is necessary to synthesize more complexes containing heterometallic bonding and explore the essential features of metallic interaction [26,27], particularly the contributions of π back-donation from transition metals to heavy main group atoms.

Recently, we isolated a silylene–germylene compound coupled through intermetallic nucleophilic substitution using a germylene anion [28]. Now we further develop a new lithium germylidenide **2b** and report the successful nucleophilic attack on iron halide complex CpFe(CO)$_2$I and β-diketiminato Fe^{II} chloride complex **6** producing three ferrogermylene complexes **3a**, **3b** and **4a**, and the exploration on their heterometallic bonding features.

---

[*] Corresponding authors.
E-mail addresses: liay@nwu.edu.cn (A. Li), wangwy@nwu.edu.cn (W. Wang), shiwq@ihep.ac.cn (W. Shi).

[1] These two authors contributed equally to this work.

https://doi.org/10.1016/j.cclet.2023.108691

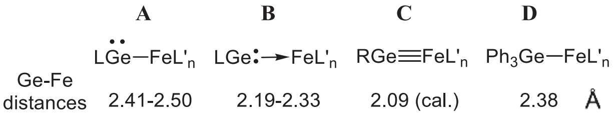

Scheme 1. Ge–Fe distances in molecules with different Ge-Fe bonding configurations.

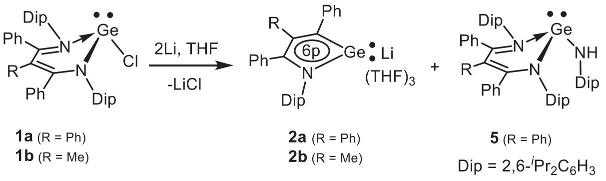

Scheme 2. Synthesis of germylidenides **2a** and **2b**.

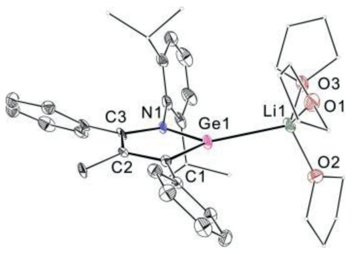

Fig. 1. Molecular structure of **2b** (CCDC: 2183919). Thermal ellipsoids are drawn at 30% probability level (except the C atoms of the ^{i}Pr groups and THF molecules). H atoms are omitted for clarity. Selected bond lengths (Å) and angles (deg): Ge1–N1 1.833(7), Ge1–C1 1.887(8), Ge(1)–Li(1) 2.688(16), N(1)–C(3) 1.447(10), C(1)–C(2) 1.374(12), C(2)–C(3) 1.427(12); N(1)–Ge(1)–Li(1) 129.4(4), C(3)–Ge(1)–N(1) 86.3(3), C(3)–Ge(1)–Li(1) 143.3(5).

The β-diketiminato germylene chlorides **1a** [29] and **1b** [30] (Scheme 2) were proved accessible in our previous work. Their further reduction reactions with lithium furnished lithium germylidenides **2a** [28] and **2b**, respectively, and the isolable byproduct **5** (Scheme 2) [31]. The new lithium germylidenide **2b** was structurally characterized by NMR spectroscopy and XRD analysis. The molecular structure of **2b** (Fig. 1) confirms a highly similar structure with that of **2a**. The Ge atom lies within a five-membered C_3NGe-ring and coordinates end-on to the Li^+ cation, which is further coordinated by three THF molecules to reach a tetrahedral coordination sphere. This is different from the structures of side-on coordinated germylidenide salts in earlier reports [32–38]. A singlet at $\delta = -0.56$ ppm in the ^{7}Li NMR spectrum of 2b is very close to that of the known lithium germylidenides **2a** ($\delta = -0.53$) [26].

Salt metathesis reactions of germylidenides **2a** and **2b** with electrophilic iron halide complex $FeCp(CO)_2I$ gave the Ge–Fe bonded complexes **3a** and **3b** in moderate isolated yields (Scheme 3). Two iron complexes were comprehensively characterized by ^{1}H and ^{13}C NMR spectroscopy, elemental analysis, and X-ray crystallography. In practice, **3a** and **3b** have the similar ^{1}H NMR spectra in C_6D_6, in which, the characteristic singlets at $\delta = 4.00$ and $\delta = 3.97$ ppm are assigned to the respective cyclopentadienyl attached to the iron atom. Nevertheless, the ^{1}H NMR spectrum of **3b** displays one set of singlet at $\delta = 2.25$ ppm for protons on the γ-C methyl group. The important chemical shifts for CO and Cp groups in the ^{13}C NMR spectra of **3a** and **3b** are very similar with the value of the reported Ge-Fe complex (δ for CO: **3a**: $\delta = 214.8$ ppm, **3b**: 215.0 ppm, (Piso)GeFeCp(CO)$_2$: 216.5 ppm, Piso$^-$ = [ArNC(^{t}Bu)NAr]$^-$; δ for Cp: **3a**: 83.5 ppm, **3b**: 83.3 ppm, (Piso)GeFeCp(CO)$_2$: 84.5 ppm) [4]. In the IR spectra of **3a** and **3b**, the absorption of stretching vibrations of carbonyls (**3a**: $\tilde{\nu} = 2019$ and 1967 cm^{-1}; **3b**: $\tilde{\nu} = 2013$ and 1959 cm^{-1}) are uniform to each other, but higher than those (1964 and 1921 cm^{-1}) of (Piso)GeFeCp(CO)$_2$, thus indicating that molecules **3a** and **3b** have weaker Fe→CO back-donation and possess more electron-poor valence shell on Fe. Furthermore, the UV–vis spectra of **3a** and **3b** in hexane severally display strong absorption bands at $\lambda = 618$ and 602 nm, respectively.

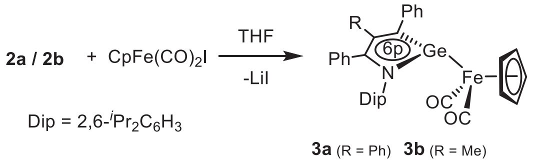

Scheme 3. Synthesis of iron-germylenes **3a** and **3b**.

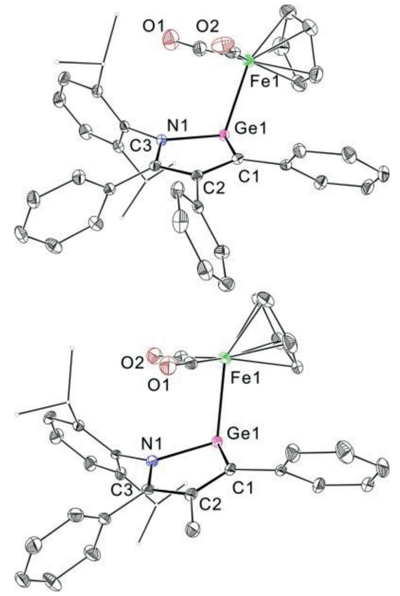

Fig. 2. Molecular structures of **3a** (CCDC: 2183920) and **3b** (CCDC: 2183921). Thermal ellipsoids are drawn at 30% probability level (except the C atoms of the ^{i}Pr groups). H atoms are omitted for clarity. Selected bond lengths [Å] and angles [deg]. **3a**: Ge(1)–Fe(1) 2.4142(5), Ge(1)–N(1) 1.9571(18), C(3)–N(1) 1.350(3), C(3)–C(2) 1.431(3), C(2)–C(1) 1.387(3), Ge(1)–C(1) 1.940(2), O(1)–C(34) 1.147(3), O(2)–C(35) 1.149(3), Fe(1)–C(35) 1.760(3), Fe(1)–C(34) 1.765(3), C(1)–Ge(1)–Fe(1) 113.43(7), N(1)–Ge(1)–Fe(1) 114.35(6), C(1)–Ge(1)–N(1) 84.01(9), C(3)–N(1)–Ge(1) 111.64(14), C(1)–C(2)–C(3) 115.2(2), N(1)–C(3)–C(2) 115.6(2), C(2)–C(1)–Ge(1) 111.33(16); **3b**: Ge(1)–Fe(1) 2.4415(11), Ge(1)–N(1) 1.995(5), C(3)–N(1) 1.337(7), C(3)–C(2) 1.442(8), C(2)–C(1) 1.379(8), Ge(1)–C(1) 1.944(6), O(1)–C(29) 1.149(8), O(2)–C(30) 1.155(8), Fe(1)–C(29) 1.755(7), Fe(1)–C(30) 1.755(7), N(1)–Ge(1)–Fe(1) 109.99(14), C(1)–Ge(1)–Fe(1) 105.78(17), C(1)–Ge(1)–N(1) 82.9(2), C(2)–C(1)–Ge(1) 113.3(4), C(1)–C(2)–C(3) 114.1(5), N(1)–C(3)–C(2) 116.7(5), C(3)–N(1)–Ge(1) 111.7(4).

The dark green crystals of **3a** and **3b** in the same monoclinic space group $P2_1/c$ were obtained from the respective concentrated hexane solutions. The corresponding molecular structures are depicted in Fig. 2. There are two independent molecules in the structure cell of **3b** that have no significant geometric differences, so only one metric parameter is discussed. The molecular structures of **3a** and **3b** confirm the three-coordinate environment of the Ge centers. A cyclopentadienyl ligand, two carbonyls, and the anionic germylene ligand are coordinated to the Fe atoms of **3a** and **3b**. In contrast with planar five-membered C_3NGe-rings of the precursors **2a** and **2b**, ferrogermylene complexes **3a** and **3b** exhibit distorted pyramidal Ge centers and slightly puckered five-membered C_3NGe-rings. The angles between the Ge-Fe bond and the Ge1-C1-N1 plane (**3a**: 123.0° and **3b**: 114.4°) are larger than those in reported digermylenes with the same azadiene anion L$^-$ of **3a** (LGe–GeL), and smaller than that

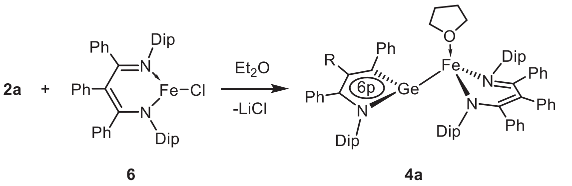

Scheme 4. Synthesis of the new low-coordinate Ge-Fe σ-complex **4a**.

in **2a**. The azadiene C_3N backbone of the five-membered heterocycles in **3a** and **3b** are nearly planar, but Ge atoms are out of planes by 12.7° and 9.3°, respectively. The negative nucleus-independent chemical shift values [NICS(1) for the C_3NGe-ring in **3a**, -11.6; in **3b**, -10.5] confirm the aromatic C_3NGe-rings in two compounds, which can provide delocalized molecular orbitals on Ge side for a further π overlap with d orbitals of Fe and improve the electronic exchange during the metallic bonding. Therefore, the Ge-Fe distances in **3a** and **3b** are just related to the metallic Ge-Fe bond. The Ge–Fe bond lengths in **3a** (2.4142(5) Å) and **3b** (2.4415(11) Å) are comparable to those in reported species (Piso)GeFeCp(CO)$_2$ (2.442 Å, Piso$^-$ = [ArNC(^{t}Bu)NAr]$^-$), and (^{Ar}Nacnac)GeFeCp(CO)$_2$ (2.496 Å, Ar=2,6-^{i}Pr$_2$C$_6$H$_3$) [4,5], but obviously longer than those in germylene→Fe complexes **B** [2,8–11] and the corresponding distances in ferrogermane derivatives **D** [39–41]. The Ge-Fe bond length in **3b** is around 3 pm longer than that in **3a**, indicating an accurate adjustment of electron density in molecular orbitals during bonding. Different from two phenyls and an electron-donating methyl on azadiene backbone of **3b**, the electron-withdrawing effect of three phenyl groups of **3a** can help to bring about the slightly electron-poor C_3NGe-ring. This should enhance the π back-donation from the **3d** shell of Fe to the π^* molecular orbitals of C_3NGe-ring and cause a little stronger Ge-Fe interaction in **3a** than that in **3b**, although this π backbonding is actually weak in both molecules. In fact, the Ge-Fe interactions only lead to a very slight difference in the C–O bond lengths of 1.147(3) and 1.149(3) Å in **3a**, as well as 1.149(8) and 1.155(8) Å in **3b**. The fact of longer Ge-N bond lengths of **3a** (1.9571(18) Å) and **3b** (1.995(5) Å) than those in precursors **2a** (1.891(2) Å) and **2b** (1.833(7) Å) should also be due to the Ge←Fe π backbond.

Very recently, we introduced a facile preparative procedure to obtain a three-coordinate β-diketiminato Fe^{II} chloride **6** (Scheme 4) [42]. The reaction of **6** with lithium germylidenide **2a** furnished the novel low-coordinate Ge^I-Fe^I complex **4a**, which has been isolated in the form of brownish red crystals in 43% yield. On the other hand, the reaction of **2b** with **6** led to a mixture of unknown products. The iron complex **4a** was completely characterized by ^1H and ^{13}C NMR spectroscopy, elemental analysis, and X-ray crystallography. According to the ^1H NMR spectrum of **4a**, the found proton integrals can be assigned for the azadiene ligand, the β-diketiminate ligand and one THF molecule, and they are not the proton resonances for precursors **2a** and **6**.

Compound **4a** crystallizes in the triclinic space group P$\bar{1}$ and exhibits a distorted tetrahedral Fe-centered coordination sphere with the heterometallic Ge→Fe bond (Fig. 3). Additionally, two N atoms of the β-diketiminate ligand and an oxygen of THF molecule are coordinated with the Fe atom, resulting in a total of 14 valence electrons centered on Fe. The interior angle summation (539.9°) of C_3NGe ring in **4a** is almost equal to that of the planar pentagonum (540°), indicating a planar five-membered ring. Contrary to **3a** and **3b**, the coordinatively unsaturated Fe1 center in **4a** is nearly coplanar with the C_3NGe plane, only exhibiting a bent angle of 18.5°. Furthermore, the six-membered C_3N_2Fe ring of **4a** presents a twist-boat conformation along the Fe1-C5 axis. The Ge1–Fe1 distance of 2.5120(6) Å is evidently longer not only than the corresponding distances in germylene→Fe complexes **B** (2.19–2.33 Å), but also than those in **3a** and **3b**. This is mainly attributed to the electron deficient Fe atom in **4a**, which leads to the weaker π back-donation from Fe to C_3NGe ring. Similarly, the bond lengths of Fe1-N2 (1.987(3) Å) and Fe1-N3 (2.027(3) Å) in **4a** are also elongated than those (both of 1.960 Å) in precursor **6**, whose absolute planar C_3N_2Fe ring has a better π-delocalization due to the coordination character of β-diketiminate ligand. The structural distinctions such as central bond lengths and bent conformation indicate that the Ge-Fe bond in **4a** is not a simply heterometallic Ge^I-Fe^I σ coordination.

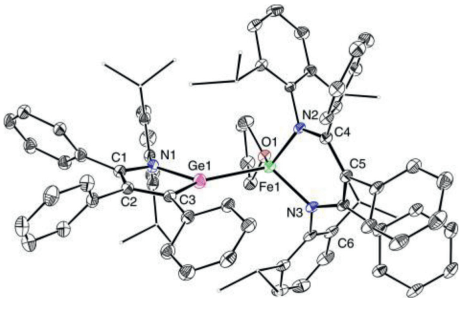

Fig. 3. Molecular structure of **4a** (CCDC, 2,236,830). Thermal ellipsoids are drawn at 30% probability level (except the C atoms of the ^{i}Pr groups). H atoms are omitted for clarity. Selected bond lengths [Å] and angles [deg]: Ge(1)-Fe(1) 2.5120(6), Ge(1)-C(3) 1.864(4), Ge(1)-N(1) 1.873(3), Fe(1)-N(2) 1.989(3), Fe(1)-N(3) 2.028(3), Fe(1)-O(1) 2.085(2), C(3)-Ge(1)-N(1) 87.74(13), N(2)-Fe(1)-N(3) 91.59(11).

The selected molecular orbitals (MOs) of **3a**, **3b** and **4a** by DFT calculations are shown in Fig. 4. A delocalized molecular orbital on the C_3NGe-ring of **3a** has a stable energy level of -4.24 eV, and is found to be the HOMO. The σ bonding characteristics are clearly visible in the portion of the HOMO-13 distributed between Ge and Fe. The HOMO and HOMO-7 of **3b** are very similar to those of **3a**. Additionally, HOMO-6 of **3b** also has a significant distribution

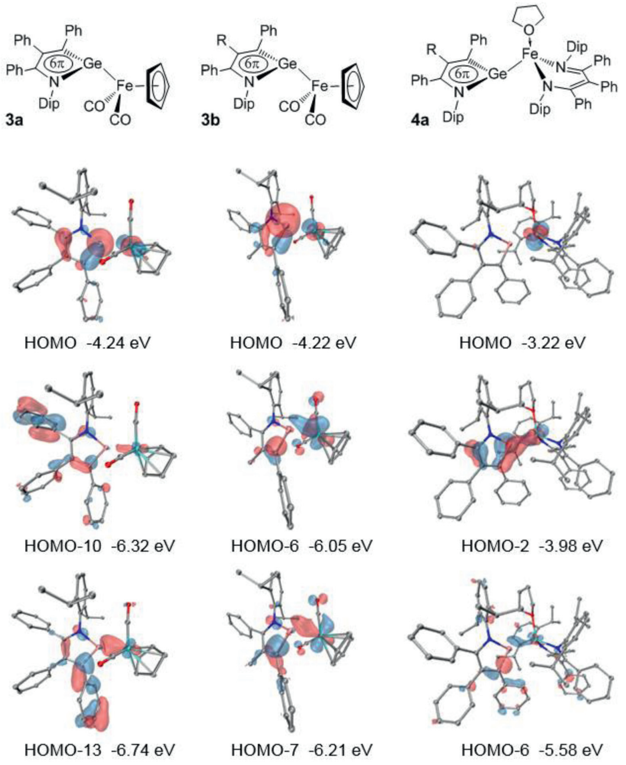

Fig. 4. Selected frontier molecular orbitals and their energy states of **3a**, **3b** and **4a** at the M06–2x/def2-TZVP level.

between Ge-Fe, but its characteristics are distinct from HOMO-7, while it is comparable to π type. This π-like orbital properties are also reflected in the HOMO-10 of the **3a**. The contribution of Fe to these bonding orbitals displays *d* orbital characters, despite the deformed shape of the molecular orbitals. Different from **3a** and **3b**, the HOMO of **4a** located at Fe atom, while the HOMO-2 derives from the overlap of the delocalized molecular orbital on the C_3NGe ring and one *d* orbital of Fe. This is most likely caused by the closeness of Fe and C_3NGe-ring to a plane, which induces a wider delocalization and what can be regarded as a π backbonding from Fe to Ge. Moreover, HOMO-6 presents a σ bonding interaction between the Ge and Fe atoms, and its energy level is -5.58 eV, which is somewhat higher than the σ type orbitals of **3a** and **3b**.

In conclusion, new ferrogermylene complexes **3a**, **3b** and **4a** have successfully been isolated by the salt metathesis reaction of lithium germylidenides with electrophilic iron halide complex $CpFe(CO)_2I$ and β-diketiminato Fe^{II} chloride, respectively. The crystal structures of new compounds show clearly that the type of ferrogermylenes A have very long heterometallic Ge-Fe bond lengths, which are affected by the changes of the coordination environment around Ge and Fe centers. The structural and IR characterizations suggest that only by accepting the presence of the Ge←Fe π back-donation in molecules **3a**, **3b** and **4a**, the observation of Ge-Fe bond lengths dependence on different ligand substituents can be reasonably explained. The computational works of **3a**, **3b** and **4a** on frontier molecular orbitals and their comparison of energy states confirmed that the Ge-Fe interactions in these molecules feature the specific σ and π mixed heterometallic bonding orbitals. Owing to coordinatively unsaturated Fe center with only 14 VE, **4a** presents a much weaker Ge←Fe π bonding contribution than those in **3a** and **3b**. Altogether, the elongation of Ge-Fe bond lengths in ferrogermylene molecules means the simultaneous diminished Ge→Fe σ donation and Ge←Fe π backbonding, not just establishing the heterometallic σ bond without the π backbond.

Declaration of competing interest

The authors declare that they have no known competing financial interests or personal relationships that could have appeared to influence the work reported in this paper.

Acknowledgments

This work was supported by National Science Foundation of China (No. 22273072), the Shaanxi Provincial Enterprise Joint Fund (No. 2021JLM-31) and the Natural Science Basic Research Plan in Shaanxi Province of China (No. 2021JM-311). We thank the measurement of crystals on Bruker D8 VENTURE PHOTON II diffractometer. The calculations were performed at the National Demonstration Center for Experimental Chemistry Education (Northwest University).

Supplementary materials

Supplementary material associated with this article can be found, in the online version, at doi:10.1016/j.cclet.2023.108691.

References

[1] M. Asay, C. Jones, M. Driess, Chem. Rev. 111 (2011) 354–396.
[2] L. Álvarez-Rodríguez, J.A. Cabeza, P. García-Álvarez, D. Polo, Coord. Chem. Rev. 300 (2015) 1–28.
[3] L.H. Pu, B. Twamley, S.T. Haubrich, et al., J. Am. Chem. Soc. 122 (2000) 650–656.
[4] C. Jones, R.P. Rose, A. Stasch, Dalton Trans. (2008) 2871–2878.
[5] S. Inoue, M. Driess, Organometallics 28 (2009) 5032–5035.
[6] X.X. Zhao, T. Szilvási, F. Hanusch, et al., Angew. Chem. Int. Ed. 61 (2022) e202208930.
[7] H. Wang, Z.W. Xie, Eur. J. Inorg. Chem. (2017) 4430–4435.
[8] I. Saur, G. Rima, K. Miqueu, H. Gornitzka, J. Barrau, J. Organomet. Chem. 672 (2003) 77–85.
[9] L.W. Pineda, V. Jancik, J.F. Colunga-Valladares, et al., Organometallics 25 (2006) 2381–2383.
[10] A. Jana, P.P. Samuel, H.W. Roesky, C. Schulzke, J. Fluorine Chem. 131 (2010) 1096–1099.
[11] S. Karwasara, R.K. Siwatch, C.K. Jha, S. Nagendran, Organometallics 34 (2015) 3246–3254.
[12] T.P. Dhungana, H. Hashimoto, H. Tobita, Dalton Trans. 46 (2017) 8167–8179.
[13] K.K. Pandey, M. Lein, G. Frenking, J. Am. Chem. Soc. 125 (2003) 1660–1668.
[14] K.K. Pandey, A. Lledós, Inorg. Chem. 48 (2009) 2748–2759.
[15] K.K. Pandey, P.P. Power, Organometallics 30 (2011) 3353–3361.
[16] K.K. Pandey, C. Jones, Organometallics 32 (2013) 3395–3403.
[17] R.S. Simons, P.P. Power, J. Am. Chem. Soc. 118 (1996) 11966–11967.
[18] A.C. Filippou, A.I. Philippopoulos, P. Portius, D.U. Neumann, Angew. Chem. Int. Ed. 39 (2000) 2778–2781.
[19] A.C. Filippou, P. Portius, A.I. Philippopoulos, Organometallics 21 (2002) 653–661.
[20] A.C. Filippou, K.W. Stumpf, O. Chernov, G. Schnakenburg, Organometallics 31 (2012) 748–755.
[21] T. Fukuda, H. Hashimoto, H. Tobita, J. Organomet. Chem. 848 (2017) 89–94.
[22] H. Hashimoto, H. Tobita, Coord. Chem. Rev. 355 (2018) 362–379.
[23] T.P. Dhungana, H. Hashimoto, M. Ray, H. Tobita, Organometallics 39 (2020) 4350–4361.
[24] H. Hashimoto, K. Nagata, Chem. Lett. 50 (2021) 778–787.
[25] P. Jutzi, C. Leue, Organometallics 13 (1994) 2898–2899.
[26] X. Zhang, L. Zhang, T. Bo, et al., Chin. Chem. Lett. 33 (2022) 3527–3530.
[27] Y.S. Huang, D.D. Chen, J. Zhu, Z.M. Sun, Chin. Chem. Lett. 33 (2022) 2139–2142.
[28] Y.Y. Qin, G. Zheng, Y. Guo, et al., Chem. Eur. J. 26 (2020) 6122–6125.
[29] X.H. Lu, H.C. Cheng, Y.F. Meng, et al., Organometallics 36 (2017) 2706–2709.
[30] L.J. Jin, X.M. Wang, H.S. Ke, et al., Chin. J. Inorg. Chem. 32 (2016) 839–845.
[31] X.M. Wang, J.J. Liu, J.X. Yu, et al., Inorg. Chem. 57 (2018) 2969–2972.
[32] W.Y. Wang, S. Yao, C. van Wüllen, M. Driess, J. Am. Chem. Soc. 130 (2008) 9640–9641.
[33] W.D. Woodul, A.F. Richards, A. Stasch, M. Driess, C. Jones, Organometallics 29 (2010) 3655–3660.
[34] C. Seow, H.W. Xi, Y.X. Li, C.W. So, Organometallics 35 (2016) 1060–1063.
[35] J.N. Wei, W.X. Zhang, Z.F. Xi, Chem. Sci. 9 (2018) 560–568.
[36] J.J. Cui, Chin. J. Org. Chem. 38 (2018) 2888–2895.
[37] Y.Y. Li, H.H. Chen, L.B. Qu, R.P. Bai, Y. Lan, Chin. Chem. Lett. 30 (2019) 2249–2253.
[38] L. Han, Z.H. Yuan. X.S. Shao, X.Y. Xu, Z. Li, Chin. Chem. Lett. 34 (2023) 107868.
[39] M.A. Bush, P. Woodward, J. Chem. Soc. A (1967) 1833.
[40] M. Itazaki, M. Kamitani, Y. Hashimoto, H. Nakazawa, Phosphorus Sulfur Silicon 185 (2010) 1054–1060.
[41] N. Kano, N. Yoshinari, Y. Shibata, et al., Organometallics 31 (2012) 8059–8062.
[42] Y.Z. Li, J. Xi, J. Ferrando-Soria, et al., Dalton Trans. 51 (2022) 8266–8272.